

Received 6 September 2022, accepted 15 September 2022, date of publication 21 September 2022,
date of current version 30 September 2022.

Digital Object Identifier 10.1109/ACCESS.2022.3208365

RESEARCH ARTICLE

A Real-Time Rule-Based Energy Management Strategy With Multi-Objective Optimization for a Fuel Cell Hybrid Electric Vehicle

HAI-BO YUAN^{1,2}, WEN-JIANG ZOU¹, SEUNGHUN JUNG¹, AND YOUNG-BAE KIM¹

¹Department of Mechanical Engineering, Chonnam National University, Gwangju, 61186, South Korea

²Automotive Engineering Research Institute, Jiangsu University, Zhenjiang 212013, China

Corresponding author: Young-Bae Kim (ybkim@chonnam.ac.kr).

This work was supported in part by the National Research Foundation of Korea under Grant 2022R111A3063283.

ABSTRACT Energy management strategy (EMS) has a great impact on securing fuel cell durability, battery charge sustenance, and fuel saving in fuel cell hybrid electric vehicles (FCHEVs). This study aims to develop EMS that can be applied in real-time to satisfy above conditions. Real time power separation was performed using rule-based EMS. A genetic algorithm (GA) was implemented to calculate the optimal battery charge/discharge criterion that simultaneously satisfies the minimum hydrogen consumption rate, battery charge rate preservation, and high fuel cell efficiency. The battery charge/discharge parameter values vary according to driving patterns, and in this paper, typical suburban, urban, and highway driving conditions are considered. For the real-time application of this research method, the effectiveness was demonstrated by applying the driving conditions of unknown patterns. The effect on the initial battery SOC on EMS was analyzed, and in order to verify the superiority of this method, it was compared and analyzed with EMS results using dynamic programming and fuzzy logic under the same driving cycles. The effectiveness of this research method was verified through simulation, and it was confirmed through experiments for real-time application. Since there is a limit to the experiment using an actual fuel cell vehicle, the experiment was performed using a fuel cell and battery. This method can be applied to real fuel cell vehicles in the same way.

INDEX TERMS Battery charge sustenance, energy management, fuel cell hybrid electric vehicle, hydrogen consumption, multi-objective GA.

I. INTRODUCTION

In recent years, the energy concerns resulting from the depletion of fossil fuels and air pollution have received increasing attention, especially in the automobile industry. Given their high energy conversion efficiency, high power density, zero emissions, and environment-friendly features, polymer electrolyte membrane fuel cell (PEMFC) electric vehicles are considered as effective substitutes for traditional vehicles. With the development of hydrogen storage devices and refueling stations, these vehicles have a long mileage and short refueling time.

The associate editor coordinating the review of this manuscript and approving it for publication was Gayadhar Panda¹.

To compensate for the slow chemical response of fuel cell systems, energy storage systems (ESSs), such as battery and/or supercapacitor, are often used. ESSs not only improve the acceleration ability of vehicles and conserve their braking energy but also improve the flexibility of power distribution in a fuel cell hybrid electric vehicle (FCHEV) system. Rapid charging/discharging rate and over-discharging of the battery lead to deterioration of the battery capacity, which in turn leads to replacement of the battery. The main concerns with FCHEV systems are tied to their economic cost, sustainable operation, and system durability, which are closely related to their energy management strategy design. The authors in [1] reviewed various EMSs and advanced optimization algorithms for addressing the above issues and proposed

some recommendations for the future development of efficient EMSs.

EMS can be categorized into rule- and optimization-based EMSs. Rule-based EMSs have high practicability and low computation load. In [2], the state of charge (SOC) and power capabilities of ESSs were main parameters in designing power distribution rules. A finite state machine-based EMS was designed for fuel cell hybrid source vehicles to benefit system health and fuel economy. To mitigate the power fluctuation of fuel cell system under rule-based EMS, Lopez *et al.* [3] utilized a low-pass filter to split the power between the fuel cell and supercapacitor system. The wavelet transform algorithm was incorporated into fuzzy logic EMS to smoothen the fuel cell current change and allocate power efficiently [4]. This approach can minimize the damage brought by current fluctuation and improve fuel cell health. Wang *et al.* [5] proposed a suboptimal online power allocation strategy based on rules and classical cybernetics and found that this strategy can realize near-optimal performance much easier than dynamic programming (DP) EMS. Optimization-based EMSs can achieve a globally optimized or a suboptimal power management by applying optimization algorithms with system control objective functions and constraints. As a global optimization algorithm that achieves optimal power distribution under vehicle system constraints, DP serves as a good benchmark for other EMSs [6]. For real-time optimization, Pontryagin's minimum principle (PMP) algorithm introduces an instantaneous optimization problem instead of global optimization in an energy management system [7]. Nevertheless, the co-state value is related to the information of driving cycles and affects the adaptability of the algorithm. The equivalent consumption minimization strategy (ECMS) is a promising real-time optimization method used in hybrid power systems. Li *et al.* proposed an online adaptive ECMS to minimize the equivalent hydrogen consumption and power source degradation in fuel cell/battery/supercapacitor hybrid electric vehicle systems while ensuring battery charge sustenance and prolonging fuel cell lifetime [8]. By taking advantage of the instantaneous optimization and future prediction ability of the model predictive control (MPC) algorithm, the authors in [9] proposed an EMS based on MPC to optimally allocate power in a hybrid electric vehicle with boundaries and constraints online. However, effective mathematical models for ECMS and MPC are necessary to obtain optimal solutions. Moreover, advanced multi-objective optimization methods [10], [11], [12], [13] have been studied to mitigate the degradation of fuel cell and battery system, save fuel consumption, and keep battery charge sustaining. Recently, machine learning algorithms, such as online learning [14], reinforcement learning [15], [16], and rule learning algorithm [17], have been investigated for power management in an FCHEV system. However, the EMS using the optimal solution shows the result using simulation, and there are few real-time optimal EMS development results.

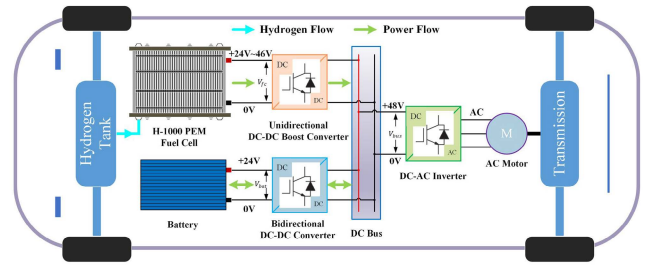


FIGURE 1. Power flow diagram of FCHEV system.

Instead of online optimization that requires big data processing, EMS with offline global optimization and real-time implementable abilities has been studied extensively for FCHEVs. The controlling parameters are optimized offline and subsequently applied online to obtain the highest practicable and optimal deterministic rules for power allocation, thereby guaranteeing online control optimality. To improve the online performance of a fuel cell hybrid power system, a rule-based EMS was developed based on the results of the dynamic programming (DP) algorithm [18]. The fuel cell system works steadily even under drastic load changes, and fuel economy optimization can be optimized like using the DP algorithm. Moreover, fuzzy logic EMS is widely combined with GA for offline optimization, and the system performance can be improved online with the optimized membership functions [19], [20], [21]. The main problem is that since global optimization is obtained based on a given driving pattern, optimal performance deteriorates when these fixed parameter values are applied to other driving cycles. To improve the adaptivity of EMS under changeable driving conditions, the authors in [22] and [23] initially optimized the parameters in different driving conditions offline and then used a driving pattern recognition method to transform the optimized membership function for real-time driving cycles.

However, the abovementioned EMSs require many control parameters to be optimized, hence this complicates the method to obtain the optimal solution and increases computation time. In addition, these EMSs are developed in a simulation or in a hardware-in-the-loop simulation and most of them lack physical experiment verification. To satisfy unknown driving pattern with the developed method, this paper presents a real-time optimized rule-based EMS that can be innovatively applied even under similar driving conditions by optimizing small number of parameters for three typical driving conditions. Simulation and experiment results reveal that the proposed EMS has a significant improvement over online rule-based EMS in terms of hydrogen consumption, fuel cell durability, and battery sustainability across each driving condition. The main contributions of this paper can be summarized as follows.

- 1) Combining multi-target GA optimization with a rule-based control strategy calculates five parameters to

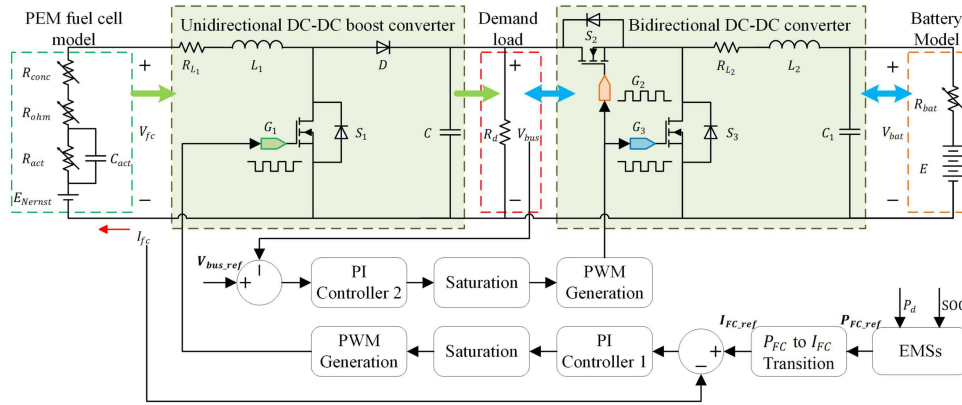


FIGURE 2. System topology of FCHEV system.

be optimized, then splits the power in the FCHEV system to achieve real-time operation with optimal performance.

- 2) Fuel consumption, fuel cell durability, efficiency, and battery sustainability are considered in a framework of multi-objective GA optimization over suburban, urban, and highway driving cycles. A Pareto analysis of multiple objectives is carried out and obtained integrated optimization parameters are used to apply to similar driving patterns to ensure reliability.
- 3) The sensitivity of the initial battery SOC value to power distribution and system performance is investigated. Results indicate that the proposed EMS can guarantee battery charge sustenance, optimizing the hydrogen consumption and improving the long driving capability of a FCHEV system.

II. ARCHITECTURE OF THE FCHEV SYSTEM

The powertrain structure of a FCHEV system is shown in Fig. 1. The PEMFC is coupled to a DC bus via a unidirectional DC-DC boost converter providing the main power supply. A battery package connected in series to a bidirectional DC-DC converter supplies extra power and recover braking energy. This topology is highly flexible because both converters achieve power control and simultaneously regulate the bus voltage. In this study, a mathematical vehicle model with real parameter information is utilized for demand power calculation. Whereas a downscaled power test platform and simulation model are constructed for energy management strategy study with downscaled demand power profiles.

A. VEHICLE MODEL

Longitudinal vehicle dynamics were modeled to obtain the vehicle running demand power [17]. The required demand power can be formulated as (1) and the main parameters are listed in Table 1.

$$P_d = mgfvcos\alpha + mgvsina + \frac{1}{2}C_dA\rho v^3 + \delta mv \frac{dv}{dt} \quad (1)$$

A DC-AC inverter, motor, and mechanical transmission system are assumed to be effective for optimization of power allocation between the fuel cell and the battery. The power balance between the power sources and demand power can be described as follows:

$$\begin{cases} P_d = P_{fc}\eta_{uni_DC} + P_{bat}\eta_{bi_DC_disc} & P_{fc} \leq P_d \\ P_d = P_{fc}\eta_{uni_DC} + P_{bat}\eta_{bi_DC_cha} & P_{fc} > P_d \end{cases} \quad (2)$$

where P_d is the demand power, P_{fc} is the fuel cell power, P_{bat} is the battery power, η_{uni_DC} is the efficiency of unidirectional DC-DC converter, $\eta_{bi_DC_cha}$ and $\eta_{bi_DC_disc}$ are the efficiency of bidirectional DC-DC converter in charge and discharge mode, respectively.

TABLE 1. Vehicle parameters.

Parameters	Description	units	value
m	Vehicle total mass	kg	1700
g	Gravitational acceleration	ms ⁻²	9.8
f	Coefficient of rolling resistance	-	0.014
α	Road slope	Degrees	0
C_d	Coefficient of air resistance	-	0.35
A	Vehicle equivalent windward area	m ²	2.59
ρ	Air density	Ns ² m ⁻⁴	1.29
δ	Weight coefficient of rotation mass	-	1.04
v	Real time vehicle speed	ms ⁻¹	-

B. PEMFC SYSTEM

A H-1000 PEMFC manufactured by Horizon Co. is applied in the FCHEV system and it provides a rated power of 1000W. As the purpose of the study is to study effectiveness of the proposed EMS, small PEMFC is utilized for the power allocation. The dynamics of a PEMFC system can be described by an equivalent electrical model with a double-layer capacitor as shown in Fig. 2. The mathematical model and specifications of a PEMFC model is demonstrated in our previous work [24].

The working efficiency of PEMFC (η_{fc}) is essential in ensuring fuel economy and cell health as defined in (3),

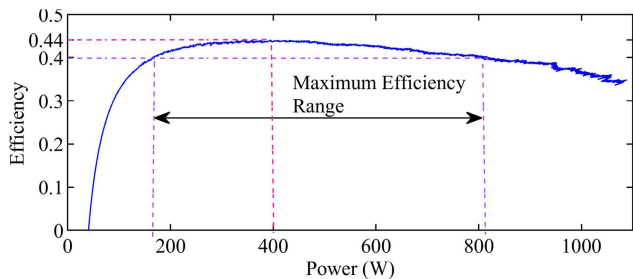


FIGURE 3. Efficiency curve of PEMFC system.

where P_{aux} is the auxiliary power consumption in the fuel cell system and HHV stands for higher heating value of hydrogen in kJ/mol . This efficiency is represented as the ratio of fuel cell net output power (P_{net}) and consumed hydrogen energy (P_{h_2}) [25]. The PEMFC efficiency curve obtained by experiment is presented in Fig. 3. The hydrogen consumption (m_{H_2}) is calculated by (4).

$$\eta_{fc} = \frac{P_{net}}{P_{h_2}} = \frac{P_{fc} - P_{aux}}{HHV \cdot \frac{NI_{fc}}{2F}} \quad (3)$$

$$m_{H_2} = \int_0^t \dot{m}_{H_2} dt = \int_0^t \frac{NI_{fc}}{2F \eta_{fc}} \cdot M_{H_2} dt \quad (4)$$

C. BATTERY

An internal resistance model with an equivalent circuit is constructed as shown in Fig. 2 to describe the dynamic characteristics of a battery. The battery output power (P_{bat}) and voltage (V_{bat}) can be calculated according to Kirchhoff's voltage law as expressed in (5). The battery current (I_{bat}) can be calculated by (6), where E represents the battery open circuit voltage (OCV) and R_{bat} is the battery internal resistance.

$$\begin{cases} p_{bat} = V_{bat} I_{bat} \\ V_{bat} = E - I_{bat} R_{bat} \end{cases} \quad (5)$$

$$I_{bat} = \frac{E - \sqrt{E^2 - 4P_{bat}R_{bat}}}{2R_{bat}} \quad (6)$$

Real-time SOC (SOC_t) can be calculated through the Coulomb counting algorithm expressed by (7), where SOC_{t_0} is the initial battery SOC, and C_b means the battery rated capacity. The battery efficiency is assumed to be 1 when charging and discharging for the simplicity.

$$SOC_t = SOC_{t_0} - \frac{1}{3600C_b} \int_{t_0}^t I_{bat} dt \quad (7)$$

D. DC-DC CONVERTERS

The bus voltage (V_{bus}) is expected to be controlled to 48V, which is higher than the output voltage range of the fuel cell and battery package. Therefore, a unidirectional DC-DC boost converter is used to regulate the fuel cell output voltage. Meanwhile, a bidirectional DC-DC converter is utilized for charging or discharging the battery. The topology using

these two types of converters is shown in Fig. 2. A constant fuel cell current is preferred during the operation because it exhibits a stable two-phase gas flow phenomenon and uninterrupted water transport through the fuel cell membrane [26]. Therefore, current mode control (CMC) of the unidirectional DC-DC boost converter is used to improve fuel cell system stability, and a proportional-integral (PI) controller 1 is applied to achieve better transient current response. The current value targeted for control is determined by the desired fuel cell power provided by the EMS. The relationship between the fuel cell current and the fuel cell power is estimated by a fitted polynomial as (8). To ensure a constant bus voltage, the bidirectional DC-DC converter takes the voltage as a control variable in the battery charging/discharging state and uses voltage mode control (VMC) with a PI controller 2. The architecture of the whole system is presented in Fig. 2, where the EMSs block is the main controller of the FCHEV system that allocates the power between the fuel cell and the battery.

$$I_{fc} = 5e - 11P_{fc}^4 - 8e - 8P_{fc}^3 + 5e - 5P_{fc}^2 + 0.0191P_{fc} + 0.2776 \quad (8)$$

In addition, the standard form of PI controller 1 and 2 is presented as (9), where u is the control variable, e is the difference between the tracked reference signal and measured process variable, K_p is the proportional gain, and T_i is the integral time.

$$u = K_p \left(e + \frac{1}{T_i} \int_0^t e dt \right) \quad (9)$$

The integral time-weighted absolute error (ITAE) method is utilized to tune the parameters of PI controllers for two designed converters, and the optimized parameters are listed in Table 2. What's more, the stability of the designed PI controllers was studied in our previous works [27], [28], and both converters can stably regulate the power output under an energy management strategy.

TABLE 2. Optimized parameters of PI controllers.

	K_p	T_i
PI controller 1	$3e-3 A^{-1}$	0.06 s
PI controller 2	$2e-4 V^{-1}$	1.2e-3 s

III. ENERGY MANAGEMENT STRATEGY ARCHITECTURE OF THE FCHEV SYSTEM

The proposed EMS combines the advantages of optimization- and rule-based EMS, aiming to optimally allocate power between two power sources of FCHEV in real time. Fuel cell durability and efficiency, minimization of hydrogen consumption, and sustainability of battery charging are considered in EMS design to ensure overall system stability and reduce operating cost. Conventional EMSs, such as DP, fuzzy logic, and rule-based EMSs are also studied to compare the advantages of the proposed EMS.

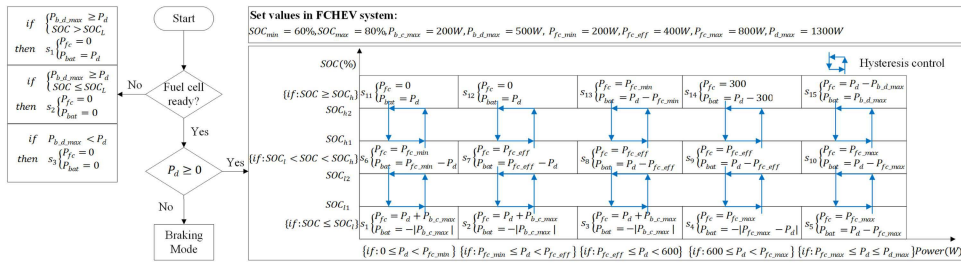


FIGURE 4. The flowchart of rule-based EMS.

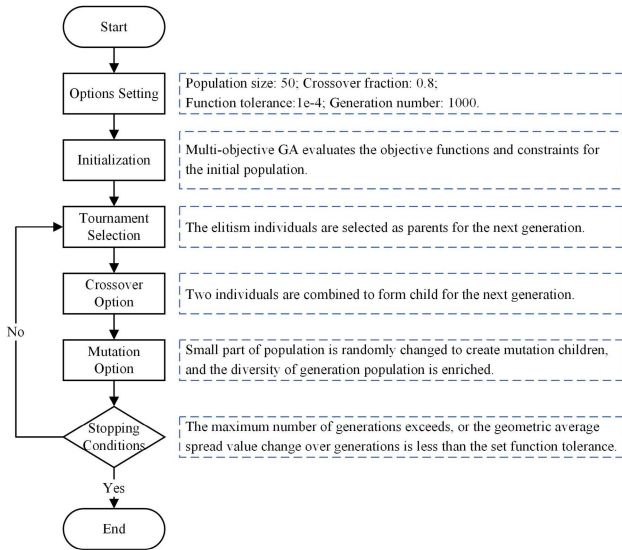


FIGURE 5. The flow chart of multi-GA optimization process.

A. RULE-BASED EMS

The core of rule-based EMS is a strategy of supplying required load power while satisfying the constraints of (10) and distributing power in real-time. The PEMFC is preferred to work in maximum efficiency range (MER) to minimize hydrogen usage as shown in Fig. 3, where the minimum fuel cell power P_{fc_min} , fuel cell power with maximum efficiency P_{fc_eff} , and maximum fuel cell output power P_{fc_max} are set to 200, 400, and 800 W, respectively. The relevant energy management rules are illustrated in Fig. 4, where the input load information is subdivided into multiple cases to design management rules because of the power limit of battery charge or discharge. Battery SOC is considered to gauge the remaining capacity of the battery and it is possible to prevent the battery from being overcharged and over-discharged, which is critical to ensure the longevity of electric vehicle system. To prevent frequent charging and discharging at the lower/upper SOC thresholds, hysteresis control is proposed in the rule-based EMS design. SOC_{l1} and SOC_{h2} denote the initial lower and upper SOC threshold values, whereas SOC_{l2} and SOC_{h1} denote the redefined lower/upper threshold values, respectively. When SOC reaches the initial lower or

upper threshold (SOC_{l1} or SOC_{h2}), the corresponding value is reassigned to the redefined value (SOC_{l2} or SOC_{h1}). The initial SOC thresholds of SOC_{l1} , SOC_{l2} , SOC_{h1} , SOC_{h2} in rule-based EMS are 60%, 65%, 70%, and 80%, respectively.

$$\begin{cases} P_{fc,min} \leq P_{fc}(k) \leq P_{fc,max} & (a) \\ P_{bat,min} \leq P_{bat}(k) \leq P_{bat,max} & (b) \\ SOC_{min} \leq SOC(k) \leq SOC_{max} & (c) \end{cases} \quad (10)$$

B. RULE-BASED EMS WITH MULTI-GA OPTIMIZATION

The power distribution in rule-based EMS is decided by the battery SOC and demand power. In general, a simple rule-based EMS gives a poor performance in terms of fuel cell durability and hydrogen consumption. Therefore, the above-mentioned concerns can be solved by multi-objective optimization using multi-GA method in this section.

1) Fuel cell durability considerations

Water flooding and membrane dehydration inside the fuel cell result in an irreversible degradation of the components including membrane, catalyst, and diffusion layer. These phenomena are mainly caused by the PEMFC’s drastic power changes and frequent start or stop operation conditions [3]. In addition, the start-up and shutdown processes of a fuel cell system lead to a rapid decay of fuel cell catalyst and diffusion layer due to imbalance pressure between cathode and anode [29]. Therefore, a low-pass filter is applied to prevent the overshoot or undershoot of the fuel cell power and to protect aging process of the fuel cell system. The effect of the cutoff frequency on the dynamics of fuel cell system is analyzed in [4], and a first-order low-pass filter with a cutoff frequency of 0.05 Hz can mitigate the power fluctuation. Moreover, PEMFC is designed to operate in non-stop driving mode that meets the minimal power threshold P_{fc_low} to avoid major performance degradation due to frequent fuel cell on-off cycling.

2) Battery charge sustaining

The battery should work under the charge sustaining mode, where the energy stored in the battery should be maintained throughout the driving cycle [30]. Sustaining battery SOC not only decelerates battery degradation [7], but also minimizes the anxiety resulting from

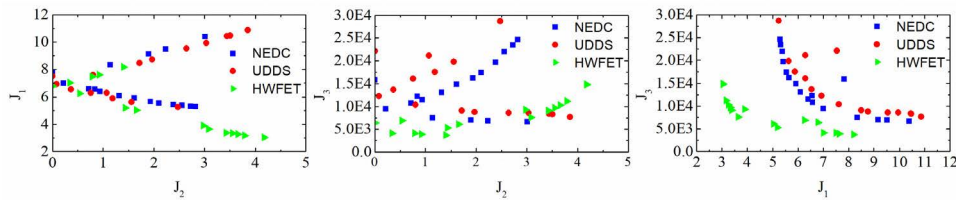


FIGURE 6. Pareto front of three objectives under three driving conditions.

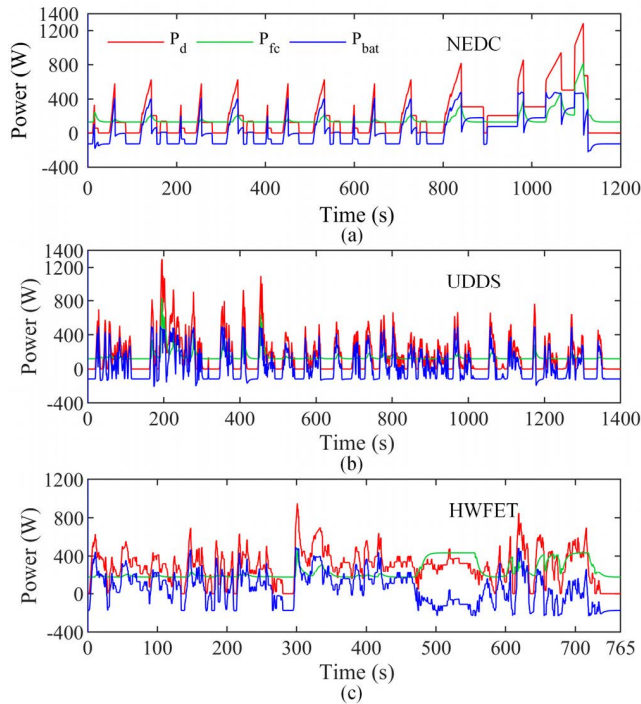


FIGURE 7. Simulation power distribution under proposed EMS ((a) NEDC; (b) UDDS; (c) HWFET).

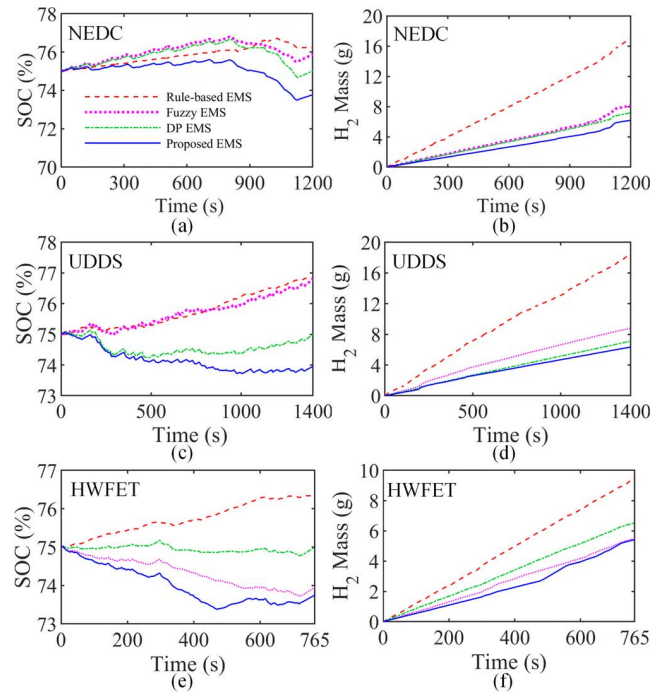


FIGURE 8. Performance comparison of simulation results under optimized driving cycles ((a) SOC variation for NEDC; (b) H_2 variation for NEDC; (c) SOC variation for UDDS; (d) H_2 variation for UDDS; (e) SOC variation for HWFET; (f) H_2 variation for HWFET).

battery overuse. The preferred battery SOC is 75% in this study.

3) Multi-objective cost function

To achieve the optimization of rule-based EMS, a multi-objective EMS combined with multi-GA optimization while having real-time operation capabilities is investigated in this section. The first cost function is the hydrogen consumption, which is calculated by (4). To guarantee the battery charge sustaining, the variation between the final and the initial SOC values ($|\Delta SOC|$) is incorporated into the objective function to determine whether the battery is over-charged or over-discharged, which is formulated by (11) (b). The acceptable SOC deviation is limited to 1.5% ($|\Delta SOC| \leq 1.5\%$), which was applied in [22] to keep battery charge sustenance. Except for two cost objectives mentioned above, a FCHEV system must meet the efficient working conditions of the PEMFC. Therefore, the third objective described in (11) (c) is targeted to

improve fuel cell efficiency and subsequently benefit fuel utilization rate. Given that it is not practical for all objectives to be optimal at the same time, a multi-objective GA is pursued to achieve a trade-off among the three objectives over a known driving cycle.

$$\begin{cases} J_1 = m_{H_2} & (a) \\ J_2 = |\Delta SOC| = |SOC_t - SOC_{t_0}| & (b) \\ J_3 = \int (0.5 - \eta_{fc}) dt & (c) \end{cases} \quad (11)$$

For three-objective optimization, the non-dominated sorting genetic algorithm II (NSGA-II) is used to find a local Pareto front for the cost functions. For each point on the Pareto front, one of the goals can only be further optimized by sacrificing the optimization of the other one or two objectives, and these points are called non-inferior solutions. A non-inferior solution is the one that provides a suitable compromise between all objectives without degrading any of them, which reveals the most appropriate trade-off among these

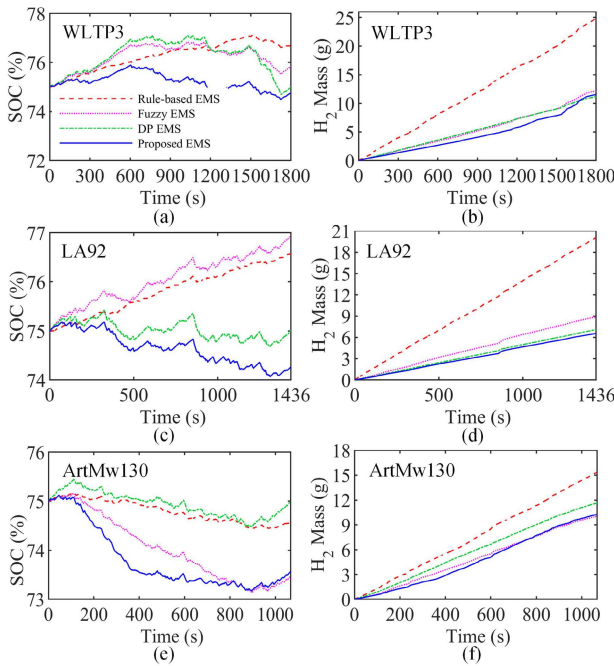


FIGURE 9. Performance comparison of simulation results under test driving cycles (a) SOC variation for WLTP3; (b) H_2 variation for WLTP3; (c) SOC variation for LA92; (d) H_2 variation for LA92; (e) SOC variation for ArtMw130; (f) H_2 variation for ArtMw130).

cost functions. In present work, the relationship between among three optimized objectives can be revealed through the method of multi-objective GA. In hysteresis control, SOC thresholds play a vital role in allocating the demand power in rule-based EMS design, which greatly affects the system performance. Hence, the parameters to be optimized are SOC_{l1} , SOC_{l2} , SOC_{h1} , SOC_{h2} , and P_{fc_low} , with the constraints listed in (12). Noting that the low limit fuel cell power P_{fc_low} considers the minimum charging power of the battery to prevent fast charging rate of the battery.

$$\begin{cases} 60\% \leq SOC_{l1} < SOC_{l2} \\ SOC_{l1} < SOC_{l2} < SOC_{h1} \\ SOC_{l2} < SOC_{h1} < SOC_{h2} \\ SOC_{h1} < SOC_{h2} \leq 80\% \\ 0 < P_{fc_low} \leq 200W \end{cases} \quad (12)$$

Multi-objective GA mimics a natural evolutionary selection process to generate a population of individual solutions repeatedly, and the optimization process is described as Fig. 5.

IV. SIMULATION RESULTS

A downscaled FCHEV system is constructed in MATLAB/Simulink. After comparing the system performance by rule-based, fuzzy logic-based, DP, and proposed EMSs, the superiority of the proposed method was emphasized. Firstly, the new European driving cycle (NEDC) for suburban driving, the urban dynamometer driving schedule (UDDS) for urban driving, and the highway federal emissions test (HWFET) for

TABLE 3. Optimized parameters for three driving conditions.

	$SOC_{l1}(\%)$	$SOC_{l2}(\%)$	$SOC_{h1}(\%)$	$SOC_{h2}(\%)$	$P_{fc_low}(W)$
NEDC	65.3285	70.3006	72.9170	75.0464	128.3791
UDDS	65.5034	70.2600	70.8782	72.4807	117.6569
HWFET	64.0369	65.9269	70.1315	73.6390	169.2560

highway driving are utilized for multi-objective GA optimization to deal with diverse road scenarios.

The optimization process is completed when the given tolerance is met. The Pareto fronts of three objectives under three driving conditions are illustrated by Fig. 6, which reveals the most appropriate trade-off among these cost functions. As can be seen from the Pareto fronts, the effects of the optimized parameters on three objective functions have coupled each other. Under three driving conditions, the trend of the relationship between any two objectives is similar except for the numerical difference. Given that an absolute variation of SOC can be derived from battery charging or discharging, the coupling among three objectives can be divided into two cases. In the case of battery charging, an increase of J_2 will lead to greater hydrogen consumption J_1 . Meanwhile, an increase of J_2 caused by battery discharging leads to less hydrogen consumption in energy management.

The proposed EMS is designed primarily to save as much hydrogen as possible while maintaining battery charge sustaining. However, due to the uncertain future driving pattern, the final SOC value is not necessarily the same as the initial value but fall within the acceptable interval. According to the Pareto front and assumed battery SOC constraint ($|\Delta SOC| \leq 1.5\%$), the final optimization parameters under three driving conditions are determined as shown in Table 3.

Under three typical driving conditions, the power distributions of a downscaled FCHEV system with EMSs are illustrated in Fig. 7. With proposed EMS, the fuel cell system operates smoothly in non-stop mode due to low power limit and low-pass filter, and the battery supports the transient power demand, which is good for fuel cell durability. With the SOC constraint, the final SOC is equal to its initial value with the DP control under three driving cycles, which are indicated by Fig. 8 (a), (c), and (e). As can be seen from Fig. 8, the proposed EMS realizes a minimum hydrogen consumption at the expense of SOC variation. In highway condition, the fuzzy EMS achieves the nearly same hydrogen consumption as the proposed EMS. However, without optimization, rule-based EMS and fuzzy-based EMS consume too much hydrogen under NEDC and UDDS, because fuel cell operates in inefficient area. In addition, the lack of optimization results in more energy being stored in the battery. During the entire driving cycle, the hydrogen consumption depends on the required fuel cell power and efficiency, which is elucidated by (4), and the proposed EMS realizes a low hydrogen consumption with admissible SOC variation.

To evaluate the adaptability of proposed EMS with unified optimization parameters under the similar driving conditions,

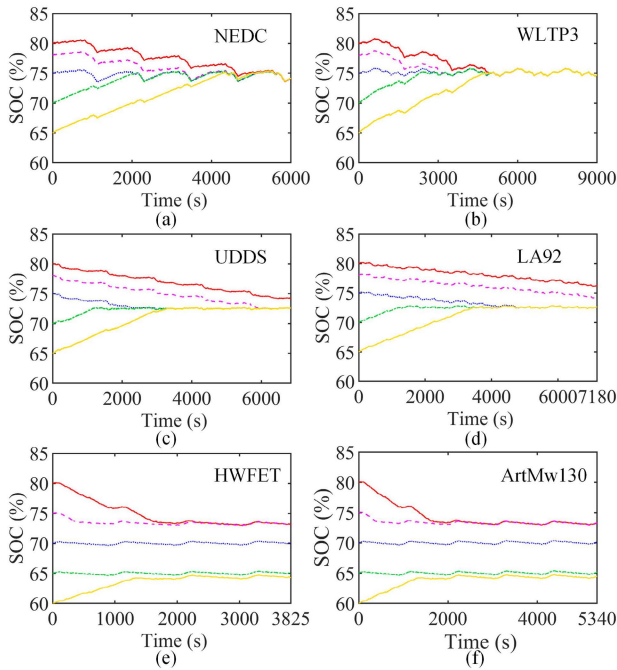


FIGURE 10. Battery SOC performance under proposed EMS in repetitive driving cycles with different initial SOC values ((a) NEDC; (b) WLTP3; (c) UDDS; (d) LA92; (e) HWFET; (f) ArtMw130).

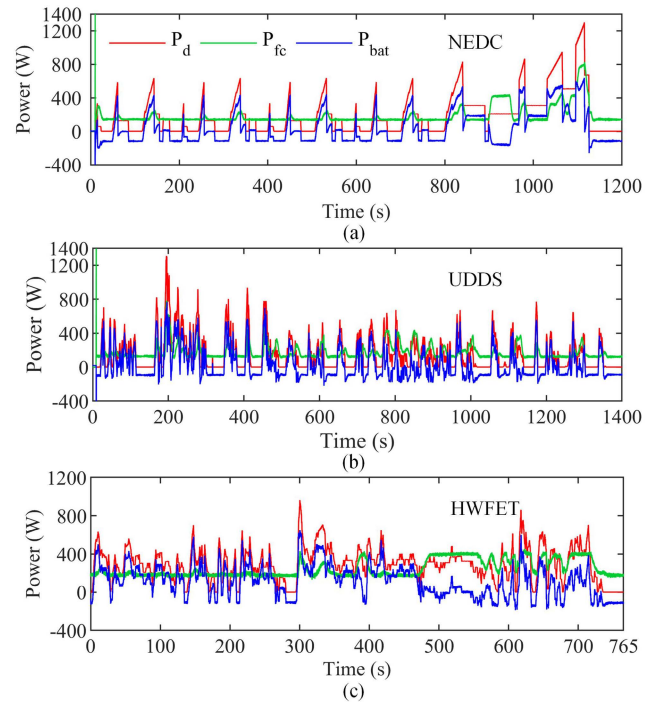


FIGURE 12. Experimental power distribution under proposed EMS ((a) NEDC; (b) UDDS; (c) HWFET).

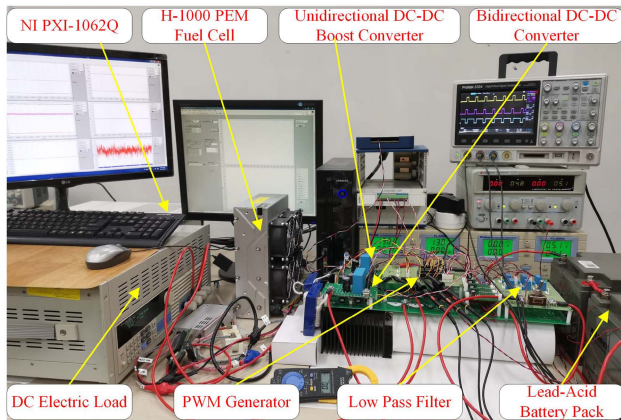


FIGURE 11. Experimental platform of PEMFC/battery hybrid power system.

the Worldwide Harmonized Light Vehicle Test Procedures class 3 (WLTP3), the California Unified Cycle (LA92), and the Artemis project Motorway driving cycle (ArtMw130) forming the test inputs, are used to validate the applicability of the proposed method. They represent different suburban, urban, and highway driving patterns, respectively, and the simulation results are presented in Fig. 9. The results show that four provided EMSs perform similarly as before in each road scenario. As the benchmark, the DP EMS achieves the optimal hydrogen consumption with battery SOC sustaining. And the proposed EMS realizes lower hydrogen consumption with acceptable SOC deviations, which validates that the optimization parameters obtained in advance can guarantee

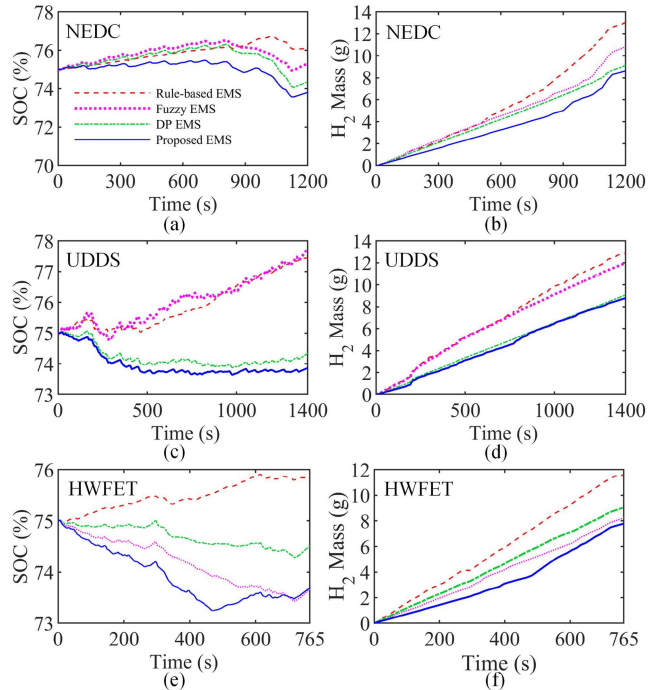


FIGURE 13. Performance comparison of experimental results under optimized driving cycles ((a) SOC variation for NEDC; (b) H_2 variation for NEDC; (c) SOC variation for UDDS; (d) H_2 variation for UDDS; (e) SOC variation for HWFET; (f) H_2 variation for HWFET).

optimal solution under the similar driving patterns, thereby proving the applicability of proposed EMS.

For fair comparison, the electric energy change caused by the final SOC variation in battery system should

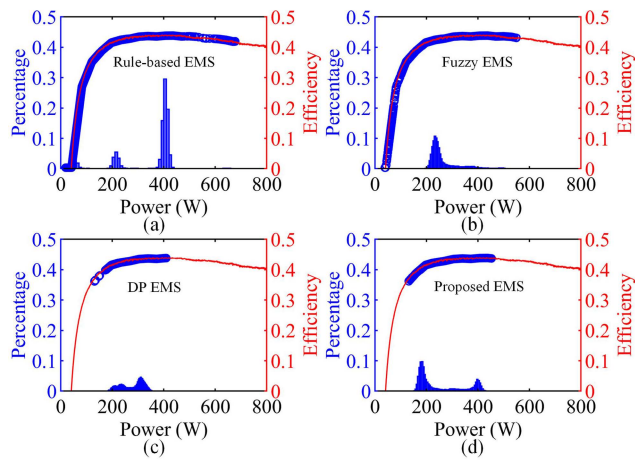


FIGURE 14. The fuel cell power distribution of different energy management strategies under driving cycle of HWFET ((a) Rule-based; (b) Fuzzy; (c) DP; (d) Proposed).

be considered. Except for the hydrogen consumption, the equivalent hydrogen consumption due to the SOC variation is calculated by the equivalent heat value [31]. The total hydrogen consumption m_{H_2-t} is given as (13), and the total hydrogen consumption comparison of different control strategies under studied driving cycles are indicated in Table 4.

$$m_{H_2-t} = m_{H_2} + \frac{\Delta SOC \cdot E_{bat} \cdot 3600}{\eta_{fc_avg} \cdot HHV} \quad (13)$$

where E_{bat} is the nominal energy capacity of the battery pack, η_{fc_avg} is the average fuel cell efficiency, and HHV expresses the higher heating value of hydrogen (MJ/kg). When SOC increases ($\Delta SOC < 0$) or decreases ($\Delta SOC > 0$), the stored or consumed energy can be converted into the equivalent decrement or increment of the hydrogen consumption.

TABLE 4. Total hydrogen consumption comparison under different energy management strategies.

Driving Cycles	Rule-based EMS (g)	Fuzzy EMS (g)	DP EMS (g)	Proposed EMS (g)
NEDC	16.006	7.6514	7.187	6.9702
UDDS	17.049	7.775	7.117	7.0356
HWFET	8.7799	6.1419	6.531	6.1319
WLTP3	23.584	11.7302	11.2	11.6789
LA92	18.678	7.774	7.104	7.0478
ArtMw130	15.6902	10.89	11.64	11.0743

As can be seen from Table 4, the proposed EMS can realize a minimal hydrogen consumption compared with DP EMS in most cases. Even though the total hydrogen consumption is not minimum under the driving cycles of WLTP3 and ArtMw130, the consumption deviation is acceptable in the face of uncertain road conditions.

To verify the ability of battery SOC sustenance, the proposed EMS is applied under the repeated driving cycles of suburban, urban, and highway with different initial SOC values. As shown in Fig. 10, with the initial SOC value of 75%, the battery SOC is maintained in an admissible range.

When the initial SOC changes, the battery SOC is automatically regulated and follows the SOC path with initial value of 75% in suburban and urban driving conditions, during which the FCHEV system is working in an optimal state. Under highway driving pattern, the battery SOC with initial value lower than 65% will finally reach to the value near 65% not 75%. When the initial SOC value is between 65% and 75%, the battery SOC will sustain near its initial value. The fuel cell does not have much power to charge the battery due to high power demand. This phenomenon is related to the optimized parameters. If they are chosen with minimum SOC deviation, the battery SOC with initial value lower than 75% will be around 75% during the driving cycle. However, the SOC recovery rate is slow due to the low charge power. In rule-based and fuzzy logic EMSs, the battery SOC greatly fluctuates due to the lack of optimization, which shortens the battery lifetime [32]. Therefore, the battery health is improved with the proposed EMS irrespective of the initial battery SOC.

V. EXPERIMENTAL VERIFICATION

A downscaled test platform is constructed to verify the effectiveness of the proposed EMS as shown in Fig. 11, and a LabVIEW-based supervisory environment is assembled for real-time monitoring. The experimental conditions are the same as those in simulation environment.

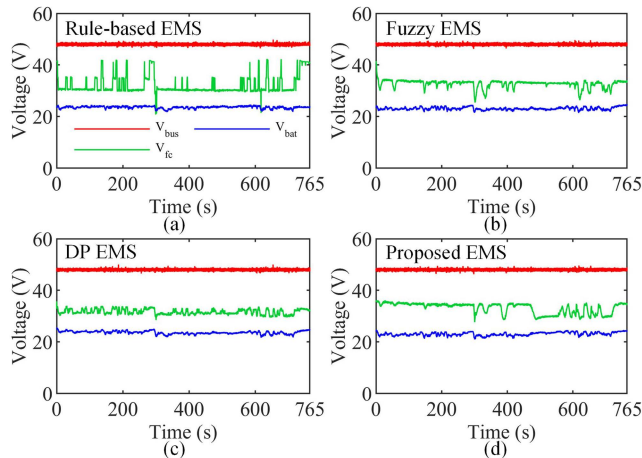
To verify the performance of the proposed EMSs in suburban, urban and highway road conditions, NEDC, UDDS and HWFET driving cycles are tested in experiment. Fig. 12 and Fig. 13 display the performance of FCHEV system with rule-based, fuzzy-based, DP and proposed EMSs. Compared with the conventional rule-based EMS under three driving patterns, the proposed EMS smoothens the fuel cell output power which makes fuel cell system work under non-stop mode, thereby benefiting for the fuel cell durability. The proposed EMS sacrifices SOC variation within an acceptable range and has a lower hydrogen consumption compared with DP EMS. The trajectories of battery SOC and hydrogen consumption in the experiment are almost identical to those observed in the simulation.

In addition, the standard deviations (std) of fuel cell power change rate under NEDC, UDDS, and HWFET in the experiment are calculated and compared to analyze the fuel cell durability, which are listed in Table 5. With proposed EMS, the fuel cell works in non-stop mode, and the output power is smoothed by the low-pass filter. Compared with rule-based EMS, the fuel cell power change rate is greatly improved with proposed EMS, even better than DP EMS under NEDC and HWFET. Under UDDS, the fuel cell provides too much low-power dynamics under the proposed EMS. Even if the hydrogen consumption is minimal, the power variation is slightly larger than that under fuzzy and DP EMSs.

To display the fuel cell power distribution in three driving conditions, the histogram of fuel cell power in HWFET is shown in Fig. 14. As shown in the figure, rule-based and fuzzy-based EMSs arrange the fuel cell to work in the less

TABLE 5. Standard derivation (std) of fuel cell power change rate under different energy management strategies.

	Rule-based	Fuzzy	DP	Proposed
	EMS (W/s)	EMS (W/s)	EMS (W/s)	EMS (W/s)
NEDC	46.1161	19.7729	17.0771	14.8314
UDDS	86.9325	23.0822	22.6533	25.6343
HWFET	59.6197	19.8819	20.3490	19.2427

**FIGURE 15. Experimental voltage response of different energy management strategies under driving cycle of HWFET (a) Rule-based; (b) Fuzzy; (c) DP; (d) Proposed).**

efficient power area, whereas DP and proposed EMSs make the fuel cell operate in MER, realizing an optimal power distribution. Under the control of proposed EMS, the fuel cell power and efficiency are well balanced, saving much hydrogen consumption.

The bus voltage V_{bus} , fuel cell voltage V_{fc} , and battery voltage V_{bat} under HWFET driving cycle are indicated by Fig. 15. Experimental results show that the output voltages of fuel cell and battery change with the driving load, while the bus voltage is adjusted well with less noise, which improves the stability of the subsequently connected devices.

VI. CONCLUSION

This paper aims to develop a practical rule-based EMS with multi-objective optimization capability in an FCHEV system. Based on the real-time power allocation ability of rule-based EMS, the multi-objective GA is applied to improve its performance through optimization with small number of parameters. Three objective functions, i.e., hydrogen consumption, battery charge sustaining, and fuel cell efficiency, are optimized offline under three typical driving conditions through multi-objective NSGA-II method. It provides a minimum hydrogen consumption relative to the DP benchmark with admissible SOC variation. The adaptability of the proposed EMS is verified in other similar three driving cycles. The sensitivity of the initial battery SOC to power management is studied systematically. As a result of this study, the proposed EMS assures that the battery can work in the optimized charging sustaining mode, which contributes to energy saving and

battery health. The rule-based EMS with multi-objective GA optimization can realize a real-time optimization for similar driving pattern. The shortcoming of this study is that it lacks online pattern recognition for unknown driving patterns to provide an optimal solution, so further study is necessary.

REFERENCES

- [1] N. Sulaiman, M. A. Hannan, A. Mohamed, P. J. Ker, E. H. Majlan, and W. R. W. Daud, "Optimization of energy management system for fuel-cell hybrid electric vehicles: Issues and recommendations," *Appl. Energy*, vol. 228, pp. 2061–2079, Oct. 2018.
- [2] Y. Wang, Z. Sun, and Z. Chen, "Energy management strategy for battery/supercapacitor/fuel cell hybrid source vehicles based on finite state machine," *Appl. Energy*, vol. 254, Nov. 2019, Art. no. 113707.
- [3] G. L. Lopez, R. S. Rodriguez, V. M. Alvarado, J. F. Gomez-Aguilar, J. E. Mota, and C. Sandoval, "Hybrid PEMFC-supercapacitor system: Modeling and energy management in energetic macroscopic representation," *Appl. Energy*, vol. 205, pp. 1478–1494, Nov. 2017.
- [4] Q. Li, W. Chen, Z. Liu, M. Li, and L. Ma, "Development of energy management system based on a power sharing strategy for a fuel cell-battery-supercapacitor hybrid tramway," *J. Power Sources*, vol. 279, pp. 267–280, Apr. 2015.
- [5] Y. Wang, Z. Sun, X. Li, X. Yang, and Z. Chen, "A comparative study of power allocation strategies used in fuel cell and ultracapacitor hybrid systems," *Energy*, vol. 189, Dec. 2019, Art. no. 116142.
- [6] W. Zhou, L. Yang, Y. Cai, and T. Ying, "Dynamic programming for new energy vehicles based on their work modes—Part II: Fuel cell electric vehicles," *J. Power Sources*, vol. 407, pp. 92–104, Dec. 2018.
- [7] K. Song, X. Wang, F. Li, M. Sorrentino, and B. Zheng, "Pontryagin's minimum principle-based real-time energy management strategy for fuel cell hybrid electric vehicle considering both fuel economy and power source durability," *Energy*, vol. 205, Aug. 2020, Art. no. 118064.
- [8] H. Li, A. Ravey, A. N'Diaye, and A. Djerdir, "Online adaptive equivalent consumption minimization strategy for fuel cell hybrid electric vehicle considering power sources degradation," *Energy Convers. Manage.*, vol. 192, pp. 133–149, Jul. 2019.
- [9] X. Li, L. Han, H. Liu, W. Wang, and C. Xiang, "Real-time optimal energy management strategy for a dual-mode power-split hybrid electric vehicle based on an explicit model predictive control algorithm," *Energy*, vol. 172, pp. 1161–1178, Apr. 2019.
- [10] M. Salem, M. Elnaggar, M. S. Saad, and H. A. A. Fattah, "Energy management system for fuel cell-battery vehicles using multi objective online optimization," *IEEE Access*, vol. 10, pp. 40629–40641, 2022.
- [11] D. Shen, C.-C. Lim, and P. Shi, "Fuzzy model based control for energy management and optimization in fuel cell vehicles," *IEEE Trans. Veh. Technol.*, vol. 69, no. 12, pp. 14674–14688, Dec. 2020.
- [12] B. Ding, Z.-X. Yang, G. Zhang, and X. Xiao, "Optimum design and analysis of flexure-based mechanism for non-circular diamond turning operation," *Adv. Mech. Eng.*, vol. 9, no. 12, pp. 1–10, 2017.
- [13] A. Khalatbarisoltani, M. Kandidayeni, L. Boulon, and X. Hu, "Power allocation strategy based on decentralized convex optimization in modular fuel cell systems for vehicular applications," *IEEE Trans. Veh. Technol.*, vol. 69, no. 12, pp. 14563–14574, Dec. 2020.
- [14] Y. Zhou, A. Ravey, and M.-C. Péra, "Multi-objective energy management for fuel cell electric vehicles using online-learning enhanced Markov speed predictor," *Energy Convers. Manage.*, vol. 213, Jun. 2020, Art. no. 112821.
- [15] X. Lin, B. Zhou, and Y. Xia, "Online recursive power management strategy based on the reinforcement learning algorithm with cosine similarity and a forgetting factor," *IEEE Trans. Ind. Electron.*, vol. 68, no. 6, pp. 5013–5023, Jun. 2021.
- [16] Z. Fu, H. Wang, F. Tao, B. Ji, Y. Dong, and S. Song, "Energy management strategy for fuel cell/battery/ultracapacitor hybrid electric vehicles using deep reinforcement learning with action trimming," *IEEE Trans. Veh. Technol.*, vol. 71, no. 7, pp. 7171–7185, Jul. 2022.
- [17] Y. Liu, J. Liu, Y. Zhang, Y. Wu, Z. Chen, and M. Ye, "Rule learning based energy management strategy of fuel cell hybrid vehicles considering multi-objective optimization," *Energy*, vol. 207, Sep. 2020, Art. no. 118212.
- [18] H. Peng, J. Li, A. Thul, K. Deng, C. Ünlübayir, L. Löwenstein, and K. Hameyer, "A scalable, causal, adaptive rule-based energy management for fuel cell hybrid railway vehicles learned from results of dynamic programming," *eTransportation*, vol. 4, May 2020, Art. no. 100057.

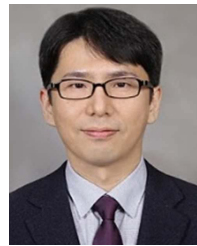
- [19] R. Zhang and J. Tao, "GA-based fuzzy energy management system for FC/SC-powered HEV considering H₂ consumption and load variation," *IEEE Trans. Fuzzy Syst.*, vol. 26, no. 4, pp. 1833–1843, Aug. 2018.
- [20] Z. Fu, L. Zhu, F. Tao, P. Si, and L. Sun, "Optimization based energy management strategy for fuel cell/battery/ultracapacitor hybrid vehicle considering fuel economy and fuel cell lifespan," *Int. J. Hydrogen Energy*, vol. 45, no. 15, pp. 8875–8886, Mar. 2020.
- [21] S. Ahmadi, S. Bathaee, and A. H. Hosseinpour, "Improving fuel economy and performance of a fuel-cell hybrid electric vehicle (fuel-cell, battery, and ultra-capacitor) using optimized energy management strategy," *Energy Convers. Manage.*, vol. 160, pp. 74–84, Mar. 2018.
- [22] J. Ryu, Y. Park, and M. Sunwoo, "Electric powertrain modeling of a fuel cell hybrid electric vehicle and development of a power distribution algorithm based on driving mode recognition," *J. Power Sources*, vol. 195, no. 17, pp. 5735–5748, Sep. 2010.
- [23] R. Zhang, J. Tao, and H. Zhou, "Fuzzy optimal energy management for fuel cell and supercapacitor systems using neural network based driving pattern recognition," *IEEE Trans. Fuzzy Syst.*, vol. 27, no. 1, pp. 45–47, Jan. 2019.
- [24] H.-B. Yuan, W.-J. Zou, S. Jung, and Y.-B. Kim, "Optimized rule-based energy management for a polymer electrolyte membrane fuel cell/battery hybrid power system using a genetic algorithm," *Int. J. Hydrogen Energy*, vol. 47, no. 12, pp. 7932–7948, Feb. 2022.
- [25] A. Kabza. (2022). *Fuel Cell Formulary*. Accessed: May 3, 2022. [Online]. Available: http://www.pemfc.de/FCF_A4.pdf
- [26] L. Xu, P. Hong, C. Fang, J. Li, M. Ouyang, and W. Lehnert, "Interactions between a polymer electrolyte membrane fuel cell and boost converter utilizing a multiscale model," *J. Power Sources*, vol. 395, pp. 237–250, Aug. 2018.
- [27] H. Yuan and Y. Kim, "Equivalent input disturbance observer-based ripple-free deadbeat control for voltage regulation of a DC–DC buck converter," *IET Power Electron.*, vol. 12, no. 12, pp. 3272–3279, Oct. 2019.
- [28] H. Yuan and Y. Kim, "Compensated active disturbance rejection control for voltage regulation of a DC–DC boost converter," *IET Power Electron.*, vol. 14, no. 2, pp. 432–441, Feb. 2021.
- [29] K. Song, H. Chen, P. Wen, T. Zhang, B. Zhang, and T. Zhang, "A comprehensive evaluation framework to evaluate energy management strategies of fuel cell electric vehicles," *Electrochim. Acta*, vol. 292, pp. 960–973, Dec. 2018.
- [30] M. Ansarey, M. S. Panahi, H. Ziarati, and M. Mahjoob, "Optimal energy management in a dual-storage fuel-cell hybrid vehicle using multi-dimensional dynamic programming," *J. Power Sources*, vol. 250, pp. 359–371, Mar. 2014.
- [31] D. Zhou, A. Al-Durra, F. Gao, A. Ravey, I. Matraji, and M. G. Simões, "Online energy management strategy of fuel cell hybrid electric vehicles based on data fusion approach," *J. Power Sources*, vol. 366, pp. 278–291, Oct. 2017.
- [32] T. Wang, Q. Li, X. Wang, Y. Qiu, M. Liu, X. Meng, J. Li, and W. Chen, "An optimized energy management strategy for fuel cell hybrid power system based on maximum efficiency range identification," *J. Power Sources*, vol. 445, Jan. 2020, Art. no. 227333.



HAI-BO YUAN received the B.S. degree in mechanical engineering from the Chongqing University of Technology, Chongqing, China, in 2015, and the M.S. degree in mechanical engineering from Chonnam National University, Gwangju, South Korea, in 2017, where he is currently pursuing the Ph.D. degree in mechanical engineering. His research interests include system identification, power converter modeling and control, PEM fuel cell modeling and control, and energy management strategy.



WEN-JIANG ZOU received the B.S. degree in vehicle engineering from the Chongqing University of Technology, Chongqing, China, in 2017, and the M.S. degree in mechanical engineering from Chonnam National University, Gwangju, South Korea, in 2019, where he is currently pursuing the Ph.D. degree in mechanical engineering. His research interests include PEM fuel cell system modeling and control, TED-CHP waste heat recovery system optimization and application, and EMS of hybrid power systems.



SEUNGHUN JUNG received the B.S. and M.S. degrees in mechanical engineering from Seoul National University, Seoul, Korea, in 2000 and 2006, respectively, and the Ph.D. degree in mechanical engineering from Pennsylvania State University, University Park, PA, USA, in 2010. In 2015, he became a Professor and founded the Electrochemical Power Laboratory, Department of Mechanical Engineering, Chonnam National University, Gwangju, Korea. He has been working on the development of multiphysics, multidimensional computational models of lithium-ion battery, and redox flow battery.



YOUNG-BAE KIM received the B.S. degree in mechanical engineering from Seoul National University, Seoul, Korea, in 1980, the M.S. degree in mechanical engineering from Korea Advanced Institute of Science and Technology (KAIST), Seoul, Korea, in 1982, and the Ph.D. degree in mechanical engineering from Texas A&M University, College Station, TX, USA, in 1990. In 1993, he joined the Mechatronics Laboratory, Department of Mechanical Engineering, Chonnam National University, Gwangju, Korea, where he became a Professor, in 2004. He published more than 150 SCI journal articles in the fuel cell and control system area. His interests include mechatronics system control, microprocessor application, and fuel cell power and control.

...